International Journal of Scientific & Engineering Research, Volume 5, Issue 3, March-2014
ISSN 2229-5518

Proposed Medical Diagnosis System Using Ripplet Transform

Hagote Kiran Kedarnath

ABSTARCT
Content based image retrieval (CBIR) approach permits the user to extract an image from a huge info based upon a matter .An economical and effective retrieval performance is achieved by choosing the only remodel and classification techniques. However, this transform techniques like Fourier transform, cosine Transform, wavelet transform suffer from discontinuities like edges in photos. to beat this disadvantage use Ripplet remodel (RT) has been enforced in conjunction with the neural network based classifier spoken as Multilayered perceptron (MLP) for locating an honest retrieval of image. Medical image fusion mistreatment pulse coupled neural network and changed abstraction frequency supported the ripplet transform. the source medical image are first decomposed by discrete RT(DRT), the low frequency sub bands (LFSs) are fused using the max selection rule. For the fusion of high frequency subbands (HFSs) a PCNN model is utilized The performance of the planned theme is evaluated by varied quantitative measures like Mutual data (MI), abstraction Frequency (SF) and Entropy (EN).

Keywords: Image Fusion, Ripplet Transform, PCNN.

I.INTRODUCTION
Advances in knowledge storage and image acquisition technologies have massive databases. therefore on alter these datas and to expeditiously manage these collections, it is necessary to develop a cost-effective image retrieval system. In Content based mostly Image Retrieval (CBIR) system the photographs could also be retrieved from large data supported the visual content data. The visual content of an image is analyzed in terms of low-level options extracted from the image. These low level options embrace color, form and texture fea. There square measure several transform techniques enforced for the feature extraction method. but the transforms techniques like Fourier remodel (FT) and moving ridge remodel (WT) suffer from discontinuities like edges and contours in pictures. so as to get rid of that standard transforms AN economical technique called Ripplet transform(RT) has been enforced for feature extraction. it's succeeding dimensional generalization of the curvelet transform, designed to represent footage at completely different scales and different directions partitioning a pair of dimensional (2D) singularities on arbitrarily formed curves. In order to boost the retrieval performance and to decrease the procedure complexities a neural network based classification tool called Multilayer perceptron (MLP) has been applied.

Recently, a theory known as Multi-scale Geometric Analysis (MGA) for high-dimensional signals has been developed, and a number of other MGA tools were planned like Ridgelet, Curvelet and Contourlet etc. These MGA tools don't suffer from the issues of ripple. Few MIF strategies supported these MGA tools were conjointly planned to boost the fusion result [7], [8]. we've got used RT within the planned methodology, as a result of it's capable of resolution 2 dimensional (2D) singularities and representing image edges additional expeditiously.

Auther:- Kiran Kedarnath Hagote, Pursing Master Degree in Information Tachnology from AVCOE Sangamner , pune university,India, Mobile +919503708183, E-mail- kirankhagote@gmail.com

However, the Importance of every supply pictures within the amalgamated image is unequal, so the way to live it and mix the corresponding coefficients became the foremost necessary drawback in MIF strategies supported MRA and/or MGA-tools. To handle this difference relating to the importance/contribution of every of the supply pictures within the amalgamated image, totally different activity level measurements (ALMs) are applied within the IF paradigm. PCNN may be a visual cortex-inspired neural network and characterized by the world coupling and pulse synchronization of neurons [9], [10]. PCNN and it's changed versions are utilized in the IF paradigm by varied researchers . The results of assorted analysis works show that PCNN outperforms the opposite standard image fusion strategies. However, in most of the present IF strategies supported PCNN, the worth of single coefficient in abstraction or transform domain is employed to inspire one vegetative cell. However a straightforward use of pixels in abstraction or remodel domain isn't effective enough as a result of humans square measure sensitive to edges and directional options. So, during this planned methodology changed abstraction frequency (MSF) within the DRT domain is employed to inspire the PCNN. The LFSs square measure amalgamated mistreatment the 'max selection' rule, and therefore the HFSs square measure amalgamated mistreatment the PCNN and MSF. each visual and quantitative performance evaluations square measure created and verified within the paper.

Performance comparisons of the proposed method with some of the existing MIF schemes, show that the proposed method performs better. The rest of the paper is organized as follows. RT is described in Section 2. In Section

International Journal of Scientific & Engineering Research, Volume 5, Issue 3, March-2014
ISSN 2229-5518

3, the standard PCNN model is briefly reviewed. Section 4, and we draw conclusion in Section 6.

II Ripplet Transform(RT)

The conventional transforms like Fourier Transform(FT) , Cosine Transform, Wavelet Transform(WT) suffer from discontinuities like edges and contours in pictures. To handle this problem, Jun XU et al. Proposed a new MGA-tool called RT. RT is a higher dimensional generalization of the Curvelet Transform (CVT), capable of representing images or 2*D* signals at different scales and different directions. To achieve anisotropic directionality, CVT uses a parabolic scaling law. From the perspective of micro local analysis, the anisotropic property of CVT guarantees resolving 2*D* singularities along *C*2 curves. On the other hand, RT provides a new tight frame with sparse representation for images with discontinuities along *Cd* curves [15].

A. Continuous Ripplet Transform (CRT)

For a two Dimensional integrable $f(\vec{x})$, the CRT is defined because the real number of $f(\vec{x})$ and ripplets as $\rho_{a\vec{b}\theta}(\vec{x})$ given in

$$R(a,\vec{b},\theta) = (\mathrm{f},\rho_{a\vec{b}\theta}) = \int f(\vec{x})\overline{\rho_{a\vec{b}\theta}(\vec{x})}d\vec{x} \qquad (1)$$

Where $R(a,\vec{b},\theta)$ are the ripplet coefficients and $\overline{(.)}$ denotes the conjugate operator. The ripplet function of the equivalent. l is defmed as

$$\rho_{a\vec{b}\theta}(\vec{x}) = \rho_{a\vec{0}\theta}(R_\theta(\vec{x}-\vec{b})) \qquad (2)$$

Where $\rho_{a\vec{0}\theta}$ is that the ripplet part perform given by the shape

$$R_\theta = \begin{bmatrix} \cos\theta & \sin\theta \\ -\sin\theta & \cos\theta \end{bmatrix} \qquad (3)$$

The equation(3) shows the rotation matrix ,where $\vec{x}$ and $\vec{b}$ are 2D vectors ; b & θ denotes the position parameter and rotation parameter severally.The ripplet part perform is defined in frequency domain as 1

$$\hat{\rho}_a(r,\omega) = \frac{1}{\sqrt{c}} a^{\frac{1+d}{2d}} \mathrm{W}(a.r)\,\mathrm{V}(\frac{a^{\frac{1}{d}}}{c.a}.\omega) \qquad (4)$$

Where $\hat{\rho}_a(r,\omega)$ is that the Fourier remodel of $\rho_{a\vec{0}\theta}$ in coordinate system, and a is that the scale parameter. W(r) is that the "radial-window" and V(ω) is the "angular window". These two windows have compact supports on [1/2 ,2] and [-1 , 1] severally. They satisfy the subsequent acceptableness conditions:

$$\int_{\frac{1}{2}}^{1} W^2(r)\frac{dr}{r} = 1 \qquad (5)$$

$$\int_{-1}^{1} V^2(t)\,dt = 1 \qquad (6)$$

Fig. The application of polar frequency domain. (The shaded 'wedge' corresponds to the frequency remodel of the part function).

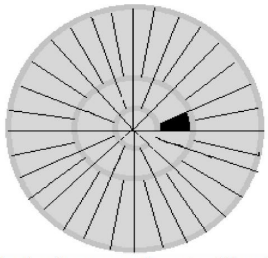

Fig.1 The tiling of polar frequency domain. (The shadowed 'wedge' corresponds to the frequency transform of the element function).

The ripplet functions decay in no time outside the elliptical effective region, that has the subsequent property for its length and width: $width \approx length^d$. Length and dimension is that the major and axis of the conic section severally. The customizable effective region tuned by support c and degree d be speaks the foremost distinctive property of ripplets (i.e) the final scaling.

The CRT will capture solely the characteristics of high frequency elements of j the size parameter 'a' cannot take the worth of infmity. So the 'full' CRT consists of fme scale RT and coarse scale isotropic WT[6]. The input perform may be reconstructed supported its ripplet coefficients.

B. Discrete Ripplet Transform (DRT)

As digital image process wants distinct transform rather than continuous remodel, here we describe the discretization of R T [6]. The discretization of CRT(Continuous ripplet remodel is based on the discretization of the parameters of ripplet functions $a_j, \vec{b_k}$ *and* θ_l substitute $a, \vec{b}, \theta$ respectively , and satisfy that $a_j = 2^{-j}, \vec{b}_k = [\mathrm{c}.2^{-j}.\mathrm{k}_1, 2^{-j/d}.\mathrm{k}_2]^T$ and $\theta_l = \frac{2\pi}{c}.2^{-[\mathrm{j}(1-1/d]}.l$, where $\vec{k} = [\mathrm{k}_1, \mathrm{k}_2]^T$,and $j,k_1,k_2,l \in \square$. $(.)^T$ denotes the transpose of a vector $d \in \square$, since any real number may be approximated by rational numbers ,so we will represent d with d=n/m and $n,m \neq 0 \in \square$. Usually, we prefer $n,m \leftarrow N$ and n; m are measure each primes. within the frequency domain, the corresponding frequency response of ripplet perform is within the type

$$\hat{\rho}_j(r,\omega) = \frac{1}{\sqrt{c}} a^{\frac{m+n}{2n}} W(2^{-j}.r)\,\mathrm{V}(\frac{1}{c}.2^{-[\mathrm{j}\frac{m-n}{n}]}.\omega - l) \qquad (7)$$

where W and V satisfy the subsequent acceptableness conditions:

$$\sum_{j=-\infty}^{+\infty} \left|W(2^{-j}.r)\right|^2 = 1 \qquad (8)$$

International Journal of Scientific & Engineering Research, Volume 5, Issue 3, March-2014
ISSN 2229-5518

$$\sum_{j=-\infty}^{+\infty}\left|\mathrm{V}(\frac{1}{c}.2^{-\lfloor j(1-1/d)\rfloor}.\omega-1)\right|^2=1 \quad (9)$$

given c ,d and j. The 'wedge' comparable to the ripplet perform within the frequency domain is

$$H_{j,l}(\mathrm{r},\theta)=\{2^j\le|r|\le 2^{2j},\left|\theta-\frac{\pi}{c}.2^{-\lfloor j(1-1/d)\rfloor}.l\right|\le\frac{\pi}{2}2^{-j}\} \quad (10)$$

The DRT of an M x N image $f(n_1,n_2)$ are within the form of

$$R_{j,\bar{k},l}=\sum_{n_1=0}^{M-1}\sum_{n_2=0}^{N-1}f(n_1,n_2)\overline{\rho_{j,\bar{k},l}(\mathrm{n}_1,\mathrm{n}_2)} \quad (11)$$

Where $R_{j,\bar{k},l}$ square measure the ripplet co-efficients. The image may be reconstructed through Inverse Discrete Ripplet Transform (IDRT)

$$f(\mathrm{n}_1,\mathrm{n}_2)=\sum_j\sum_{\bar{k}}\sum_l R_{j,\bar{k},l}\rho_{j,\bar{k},l}(\mathrm{n}_1,\mathrm{n}_2) \quad (12)$$

As a generalized version of the present curvelet transform, RT is not only capable of resolution second Dimensional singularities, but it additionally has few smart properties [7]:

1. It forms a brand new tight enclose a perform house. And is capable of localizing in spatial and frequency domain providing a additional economical and effective representation for images or 2D signals.
2. It has general scaling with impulsive degree and support that will capture second singularities on

Different curves in any directions. Jun XU et al. have showed that RT will give a more practical representation for pictures with singularities on smooth curves [6]. It outperforms DCT and rippling in Nonlinear approximation, once the quantity of preserved coefficients is little. Just in case of image denoising application, RT performs higher than curvelet and discrete rippling transform. Of these experiments show that RT primarily based image writing is appropriate for representing texture or edges in pictures.

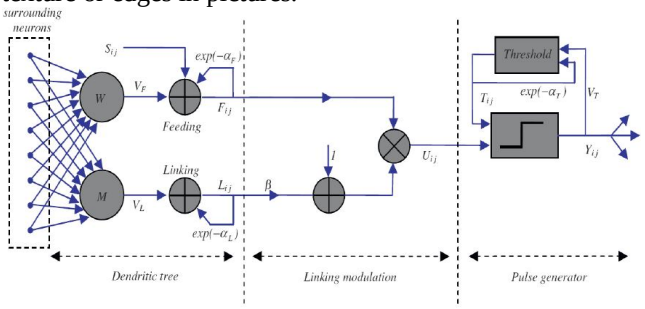

Fig. 2. Structure of PCNN.

III. PULSE COUPLED NEURAL NETWORK

PCNN may be a single stratified, two-dimensional, and laterally connected neural network of pulse coupled neurons. The PCNN neurons structure is shown in Fig. 2. The nerve cell consists of Associate in Nursing input half (dendritic tree), linking half and a generator. The nerve cell receives the input signals from feeding and linking inputs. Feeding input is that the primary input from the neurons receptive space. The nerve cell receptive space consists of the neighboring picture elements of corresponding pixel within the input image. Linking input is that the secondary input of lateral connections with neighboring neurons. The distinction between these inputs is that the feeding connections have a slower characteristic response time constant than the linking connections. the quality PCNN model is delineate as iteration by the subsequent equations [10], [16]:

$$F_{i,j}[n]=e^{-\alpha_F}F_{i,j}[\mathrm{n}-1]+\mathrm{V}_F\sum_{k,l}w_{i,j,k,l}Y_{i,j}[n-1]+S_{i,j} \quad (12)$$

$$L_{i,j}[n]=e^{-\alpha_L}L_{i,j}[n-1]+V_L\sum m_{i,j,\mathrm{k,l}}Y_{i,j}[n-1] \quad (13)$$

$$U_{i,j}[n]=F_{i,j}[n](1+\beta\ \mathrm{L}_{i,j}[\mathrm{n}]) \quad (14)$$

$$\mathrm{Y}_{i,j}[n]=\begin{cases}1, & U_{i,j}[n]>T_{i,j}[n]\\ 0, & otherwise\end{cases} \quad (15)$$

$$T_{i,j}[n]=e^{-\alpha_T}T_{i,j}[n-1]+V_TY_{i,j}[n] \quad (16)$$

In the Eq.(12) to Eq.(16), the indexes *i* and *j* seek advice from the pixel location within the image, *k* and *l* seek advice from the dislocation in an exceedingly symmetric neighborhood around one pixel, and *n* denotes the current iteration (discrete time step). Here *n* varies from one to N (total variety of iterations). The dendritic tree is given by Eqs.(12)-(13).The 2 main elements *F* and *L* area unit known as feeding and linking, severally. $w_{i,j,k,l}$ and $m_{i,j,\mathrm{k,l}}$ area unit the synaptic weight coefficients and S is that the external input. V_F And V_L area unit normalizing constants. α_F And α_L area unit the time constants; usually, $\alpha_F<\alpha_L$. The linking modulation is given in equivalent weight.(16), wherever $U_{i,j}[n]$ is that the internal state of the neuron and β is that the linking parameter. The heart beat generator determines the firing events within the model in equivalent weight.Eq.(15). $\mathrm{Y}_{i,j}[n]$ Depends on the inner state and threshold. The dynamic threshold of the nerve cell is equivalent Eq.(16), where V_T and α_T area unit normalized constant and time constant, severally.

IV. PROPOSED METHOD

The notations used in this section as follows: A, B, R represents the 2 source pictures and therefore the resultant image, severally. C = (A,B,R). L_G^C Indicates the LFS of the image C at the coarsest scale G. $D_{g,h}^C$ represents the HFS of the image C at scale g, (g = 1,….,G) and direction h. (i; j) denotes the spatial location of every coefficient . The method is simply extended to more than two pictures.

A.*Fusing Low Frequency Subbands*

The LFSs coefficients area fused using 'max selection' rule. According to this fusion rule, choose the frequency coefficients from L_G^A or L_G^B with larger definite quantity

International Journal of Scientific & Engineering Research, Volume 5, Issue 3, March-2014
ISSN 2229-5518

because the fused coefficients:

$$L_G^R(i,j) = \begin{cases} L_G^A(i,j), & \left|L_G^A(i,j)\right| \geq \left|L_G^B(i,j)\right| \\ L_G^B(i,j), & otherwise \end{cases} \quad (17)$$

B. Fusing High Frequency Sub bands

The HFSs of the supply pictures are fused PCNN. As humans area unit sensitive to options like edges, contours etc., so rather than PCNN in DRT domain directly (i.e., using individual coefficients), changed spatial frequency (MSF) in DRT domain is taken into account because the image feature to inspire the PCNN.

1) *Modified spatial Frequency (MSF)*: spatial frequency (SF) projected by Eskicioglu et al. is calculated by row and column frequency [17]. It reflects the entire activity level of an image, which implies the larger the SF, the upper the image resolution. We have used a changed version of SF within the proposed MIF technique. The MSF consists of row (RF), column (CF) and diagonal frequency (DF). For a M×N pixels image *f* the MSF is outlined as

$$MSF = \sqrt{RF^2 + CF^2 + DF^2} \quad (18)$$

Where,

$$RF = \sqrt{\frac{1}{M(N-1)}\sum_{m=1}^{M}\sum_{n=2}^{N}\left[f_{m,n} - f_{m,n-1}\right]^2} \quad (19)$$

$$CF = \sqrt{\frac{1}{(N-1)M}\sum_{m=2}^{M}\sum_{n=1}^{N}\left[f_{m,n} - f_{m-1,n}\right]^2} \quad (20)$$

And,

$$DF = P + Q \quad (21)$$

Where,

$$P = \sqrt{\frac{1}{(M-1)(N-1)}\sum_{m=2}^{M}\sum_{n=2}^{N}\left[f_{m,n} - f_{m-1,n-1}\right]^2} \quad (22)$$

And,

$$Q = \sqrt{\frac{1}{(M-1)(N-1)}\sum_{m=2}^{M}\sum_{n=2}^{N}\left[f_{m-1,n} - f_{m,n-1}\right]^2} \quad (23)$$

2) *Fusion using DRT-MSF-PCNN:* Let, $MSF_{i,j}^{g,h,C}$ be the changed spatial frequency similar to a coefficient $D_{g,h}^{C}(i,j)$, measured by using overlapping window around the involved coefficient where C = (A,B). so as to reduce the machine complexness, we tend to use a simplified PCNN:

$$F_{i,j}^{g,h,C}[n] = MSF_{i,j}^{g,h,C} \quad (24)$$

$$L_{i,j}^{g,h,c}[n] = e^{-\alpha_L} L_{i,j}^{g,h,c}[n-1] + V_L \sum_{k,l} W_{i,j,k,l}^{g,h,C} Y_{i,j,k,l}^{g,h,C}[n-1] \quad (25)$$

$$U_{i,j}^{g,h,C}[n] = F_{i,j}^{g,h,C}[n] * (1 + \beta L_{i,j}^{g,h,C}[n]) \quad (26)$$

$$\theta_{i,j}^{g,h,C}[n] = e^{-\alpha_\theta} \theta_{i,j}^{g,h,C}[n-1] + V_\theta Y_{i,j}^{g,h,C}[n-1] \quad (27)$$

$$Y_{i,j}^{g,h,C}[n] = \begin{cases} 1, & U_{i,j}^{g,h,C}[n] > \theta_{i,j}^{g,h,C}[n] \\ 0, & otherwise \end{cases} \quad (28)$$

$$T_{i,j}^{g,h,C}[n] = T_{i,j}^{g,h,C}[n-1] + T_{i,j}^{g,h,C}[n] \quad (29)$$

Where, the feeding input $F_{i,j}^{g,h,C}[n]$ up to the normalized modified spatial frequency $MSF_{i,j}^{g,h,C}$. The linking input $L_{i,j}^{g,h,c}$ is up to the total of neurons firing times in linking range. $W_{i,j,k,l}$ Is that the conjunction gain strength and subscripts k and l area unit the dimensions of linking range the PCNN. a_L is the decay constants. β Is that the linking strength, V_L and V_θ area unit the amplitude gains. $U_{i,j}^{g,h,C}$ is that the total internal activity and $\theta_{i,j}^{g,h,C}$ is that the threshold. If $U_{i,j}^{g,h,C}$ is larger than $\theta_{i,j}^{g,h,C}$, then the nerve cell can generate a pulse $Y_{i,j}^{g,h,C}$=1, is known as one firing time. The total of $Y_{i,j}^{g,h,C}$=1 in *n* iteration (namely the firing times), is employed to represent the image info. Here, instead of $Y_{i,j}^{g,h,C}[n]$, we've analyzed $T_{i,j}^{g,h,C}[n]$, since neighboring coefficients with similar options represent similar firing times in an exceedingly given iteration times.

C. Algorithm

The medical pictures to be coalesced should be registered to assure that the corresponding pixels area unit aligned. Here we tend to outlines the salient steps of the projected MIF method:

1) Decompose the registered supply medical pictures A and B by DRT to get the LFSs and HFSs.
2) Fused the coefficients of LFSs using the 'max selection' rule delineate in Section IV-A, to get the fused LFS.
3) Compute the MSF as delineate in Section IV-B1, using overlapping window on the coefficients in HFSs.
4) Input MSF of every HFSs to inspire the PCNN and generate pulse of neurons with Eqs.(24)–(29). and cypher the firing times $T_{i,j}^{g,h,C}[n]$ by equivalent weight.(31).
5) If n = N, then iteration stops. Then fuse the coefficients in the HFSs by the subsequent fusion rule:

$$D_{i,j}^{g,h,C}[n] = \begin{cases} D_{g,h}^{A}(i,j), & T_{i,j}^{g,h,A}[N] > T_{i,j}^{g,h,B}[N] \\ D_{g,h}^{B}(i,j), & otherwise \end{cases} \quad (30)$$

6) Apply inverse ripplet remodel (IDRT) on the fused LFS and HFSs to get the ultimate fused medical image. The diagram of the projected M IF theme is shown in Fig. 3.

International Journal of Scientific & Engineering Research, Volume 5, Issue 3, March-2014
ISSN 2229-5518

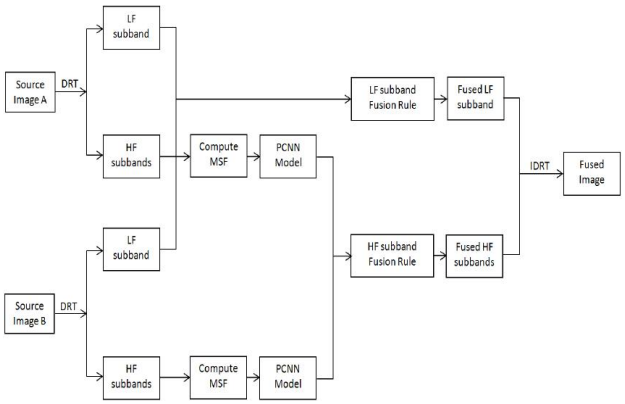

Fig. 3. Diagram of the projected MIF technique.

V. Conclusion

We propose a novel multimodality MIF method based on ripplet transform using modified spatial frequency motivated PCNN. The DRT is capable of resolving two dimensional singularities and representing image edges more efficiently, which makes the fused images clearer and more informative. To integrate as much information as possible into the fusedimages the low frequency source subbands are fused using 'max selection' rule, and PCNN is used to select the 'better' coefficients from the decomposed source high frequency subbands. To improve the result, instead of using single coefficient to motivate the PCNN, modified spatial frequency is used as the image feature to motivate the PCNN.

ACKNOWLEDGMENT

We would like to thank Jun Xu and Depeng Wu (Dept. of Electrical and Computer Engineering, University of Florida, USA) for helping us in the implementation of Ripplet Transform.

REFERENCES

[1] Barra V. and Boire,J.Y "A general framework for the fusion of anatomical and functional medical images," *NeuroImage*, vol. 13, no. 3, pp. 410–424, 2001.
[2] Yonghong J., "Fusion of landsat TM and SAR image based on principal component analysis," *Remote Sensing Technology and Application*, vol. 13, no. 1, pp. 46–49, 1998.
[3] Li S. and Yang B., "Multifocus image fusion using region segmentation and spatial frequency," in *Proc. of Image Vision Computing*, vol. 26, no. 7, 2008, pp. 971–979.
[4]. Li H, B. S. Manjunath, and S. K. Mitra, "Multi-sensor image fusion using the wavelet transform," in *Proc. of CVGIP: Graphical Model and Image Processing*, vol. 57, no. 3, 1995, pp. 235–245.
[5] Liu Q., ping Xu L., Wang Y., Ma Y. de, and Xie Q., "A novel algorithm of image fusion based on adaptive ULPCNN time matrix," in *Information Engineering (ICIE), 2010 WASE International Conference on*, vol. 1, aug. 2010, pp. 198 –202.
[6] Xiao-Bo Q., Jing-Wen Y., Hong-Zhi X., and Zi-Qian Z., "Image fusion algorithm based on spatial frequency-motivated pulse coupled neural networks in nonsubsampled contourlet transform domain," *Acta Automatica Sinica*, vol. 34, no. 12, pp. 1508–1514, 2008.
[7] Wang Z, Ma Y., and Gu J., "Multi-focus image fusion using PCNN," *Pattern Recognition*, vol. 43, no. 6, pp. 2003–2016, June 2010.
[8] Wang Z. and Ma Y., "Medical image fusion using m-PCNN," *Information Fusion*, vol. 9, no. 2, pp. 176–185, April 2008.
[9] J. Xu, L. Yang, and. Wu D, "Ripplet: A new transform for image processing," *Journal of Visual Communication and Image Representation*, vol. 21, no. 7, pp. 627–639, 2010.
[10] Johnson J. and Padgett M., "PCNN models and applications," *Neural Networks, IEEE Transactions on*, vol. 10, no. 3, pp. 480 –498, may 1999.
[11] Eskicioglu A. and Fisher P., "Image quality measures and their performance," *Communications, IEEE Transactions on*, vol. 43, no. 12, pp. 2959 –2965, Dec 1995.
[12] G. H. Qu, D. L. Zhang, and P. F. Yan, "Information measure for performance of image fusion," *Electronic Letters*, vol. 38, no. 7, pp. 313–315, 2002.